



Buried plastic scintillator muon telescope

F. SANCHEZ¹, G. A. MEDINA-TANCO¹, J. C. D'OLIVO¹, G. PAIC¹, M. E. PATINO SALAZAR¹, E. NAHMAD-ACHAR¹, J. F. VALDES GALICIA², A. SANDOVAL³, R. ALFARO MOLINA³, H. SALAZAR IBARGUEN⁴, M. A. DIOZCORA VARGAS TREVINO⁵, S. VERGARA LIMON⁵, L. M. VILLASENOR⁶.

¹ Instituto de Ciencias Nucleares, Universidad Nacional Autónoma de México, México, D.F., C.P. 04510,

² Instituto de Geofísica, Universidad Nacional Autónoma de México, México, D.F., C.P. 04510,

³ Instituto de Física, Universidad Nacional Autónoma de México, México, D.F., C.P. 04510,

⁴ Instituto de Física, Universidad de Puebla, México, Puebla, C.P. 72570,

⁵ Facultad de Ciencias de la Electrónica, Grupo de Robótica, Benemérita Universidad Autónoma de Puebla, Av. San Claudio y 18 Sur C. U., Edif. 182, C.P. 72570, Puebla, México,

⁶ Universidad de Michoacan, Morelia, Mich., C.P. 58040, México.

federico.sanchez@nucleares.unam.mx

Abstract: Muon telescopes have several applications, ranging from astrophysics to fundamental particle physics. We show the design parameters, characterization and end-to-end simulations of a detector composed by a set of three parallel dual-layer scintillator planes, buried at fix depths ranging from 0.30 m to 3 m. Each layer is 4 m² and is composed by 50 rectangular pixels of 4 cm × 2 m, oriented at a 90 deg angle with respect to its companion layer. The scintillators are MINOS type extruded polystyrene strips with two wavelength shifting fibers mounted on machined grooves. Scintillation light is collected by multi-anode PMTs of 64 pixels, accommodating two fibers per pixel. The front-end electronics has a time resolution of 7.5 nsec. Any strip signal above threshold opens a GPS-tagged 2 micro-seconds data collection window. Separation of extensive air shower signals from secondary cosmic-ray background muons and electrons is done offline using the GPS-tagged threefold coincidence signal from surface water cerenkov detectors located nearby in a triangular array. Cosmic-ray showers above 6 PeV are selected. The data acquisition system is designed to keep both, background and signals from extensive air showers for a detailed offline analysis.

Introduction

The Earth atmosphere is constantly hit by the cosmic radiation. After the first interaction occurs with air molecules at high altitudes, showers of secondary particles are generated and, eventually, their products may reach the ground. The exact fraction of each product at the surface level depends on the atmospheric mass overburden but, in any case, the most important components are the muonic and the electromagnetic ones. Muons are the most numerous charged particles and are mainly produced from the decay of charged mesons at heights of around 15 km. The electromagnetic component at ground consist of electrons, positrons and photons primarily from electromagnetic cascades initiated by the decay of neu-

tral and charged mesons and followed by pair production and Bremsstrahlung. The ratio of the electromagnetic to muon component at ground carries crucial information about the primary cosmic radiation. The number of muons at ground can be used to infer the fundamental physics involved in the first interactions points as well as the mass composition of the primary particle.

The main goal of the experimental setup presented in this work is to discriminate the muonic and electromagnetic component coming from cosmic ray showers above 6 PeV and measure their ratio as a function of the underground depth. As the background muons will also be continually recorded and stored, an additional goal of the experiment is the search for muon excesses in the sky.

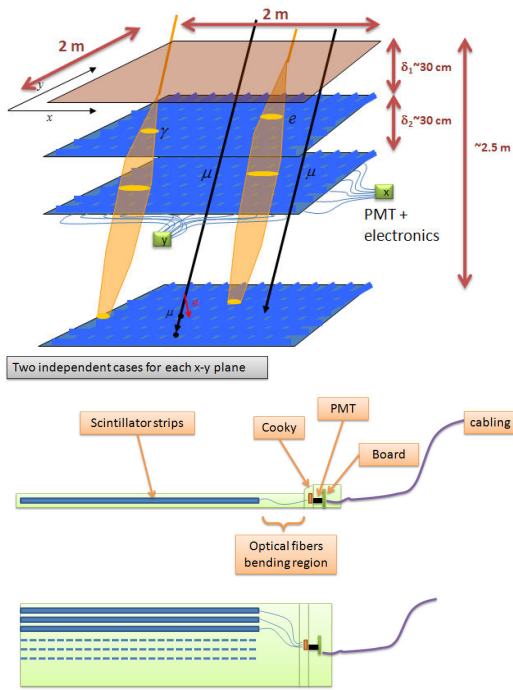


Figure 1: Schematic view of the whole detector layout (top) and casing of one scintillator layer (bottom).

Experimental setup

In order to separate muons from photons, electrons and positrons the telescope has three horizontal dual-layer scintillator planes buried at different depths (see figure 1). Each layer consists of 50 scintillator strips 2 m long, 4 cm wide and 1 cm thick. In each plane, the two layers are rotated by 90 deg in order to produce an effective x-y plane with $4 \text{ cm} \times 4 \text{ cm}$ pixels covering an area of 4 m^2 . Each scintillator strip is made of polystyrene doped with 1% PPO and 0.03% POPOP [1]. They are co-extruded with an outer layer of TiO_2 in order to improve reflectivity and have two wavelength shifting (WLS) fibers mounted on machined grooves.

The scintillator light coming from each layer is collected by multi-anode PMTs of 64 pixels (H7546B), accommodating the two fibers of each strip on a single PMT pixel. The front-end electronics has a time resolution of 7.5 nsec. A schematic view of the electronic board correspond-

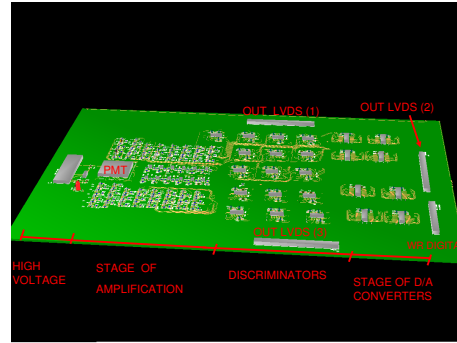


Figure 2: Schematic view of the electronic board of one detector layer. Main components are indicated.

ing to a single layer is shown in Figure 2 where its main components are indicated. Each channel contains an amplification stage prior to discrimination. The thresholds for each channel can be adjusted independently in real time. The detector will have six of such boards enclosed and buried in the same casing as the scintillator planes. Any strip signal above threshold opens a GPS-tagged 2 micro-seconds data collection window.

The three scintillator planes will be combined with a triangular array of water cerenkov detectors on the surface. The surface detectors will be 200 m apart from each other in order to produce a GPS-tagged threefold coincidence signal for cosmic ray showers of energy above 6 PeV. The separation of the background from the signal coming from showers will be performed offline.

The first two planes are planned to be buried at around 25 cm and 50 cm respectively, around the depth of maximum development for electromagnetic showers in the ground. The third plane would be buried at ~ 2.5 m. However, the actual final depths are being optimized by Monte Carlo simulations [2], in order to maximize the discrimination potential of the telescope between muon and electromagnetically originated tracks. The muons are the most penetrating charged particles that propagate underground. Since their propagation is almost linear they are expected to cross the whole telescope volume leaving a well defined single-pixel signal in the three planes. The photons, electrons and positrons, on the other hand, develop small showers underground that may leave a two-

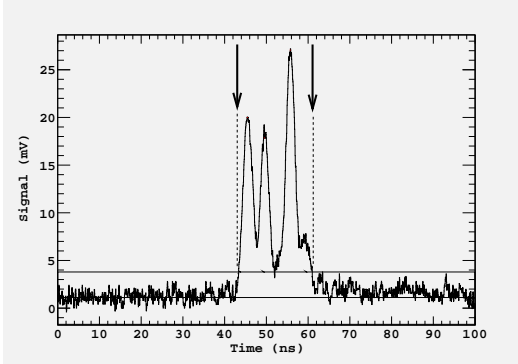


Figure 3: PMT signal from a muon in the lab with Bicron fibers. Lines indicate the mean and the 5σ noise level respectively. The trigger will fire when any signal is above 5σ .

dimensional footprint on the shallower planes of the detector.

Measurements

The scintillation light is collected at only one end of the 2 m strips and, therefore, attenuation becomes an important factor, specially for particles hitting the opposite end of the strip. To guarantee an acceptable light output, we have tested in our laboratory fibers produced by Bicron and Kuraray. The first one is known to have a better time resolution while the second one has a higher light yield. The typical time profile of a single muon signal, produced by the scintillator combined with Bicron fibers, is shown in Figure 3. It can be seen that the signal is structured, being composed in this particular case by three pulses. The total width of the signal, defined as the time difference between the first and last time the pulse is above of 5σ over background, is on the order of 20 nsec (see the arrows).

To compute the time resolution we compared for both fibers the rise time of the respective signals, defined as the lapse between the nearest 1σ level crossing preceding the time of threshold (at 5σ). We can see from Figure 4 that the mean rise times of both fibers are close to 1 nsec.

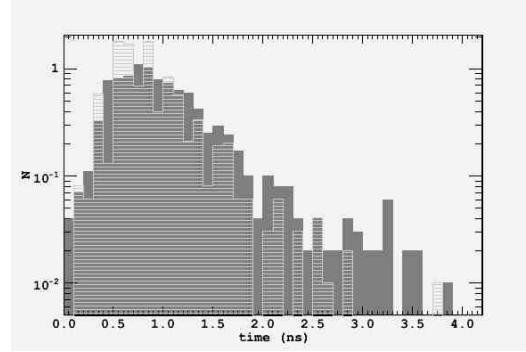


Figure 4: Rise time (see text) distribution. Solid and open histograms are with Bicron and Kuraray fibers respectively.

In order to characterize the light yield of the two types of fibers we measure in coincidence with two smaller scintillators ($\sim 10^2 \text{ cm}^2$) sandwiching the strip. This setup allows to measure the output charge for cosmic background muons as a function of the distance to the PMT. In order to reproduce the short and the long attenuation lengths, typical of WLS, we calculate the attenuation length of each type of fiber by fitting a double exponential function to the medians of the photoelectron distributions:

$$\langle phe \rangle = a_1 e^{-x/\lambda_1} + a_2 e^{-x/\lambda_2}, \quad (1)$$

with $a_1 + a_2 = \langle phe \rangle_0$. As an example, in Figure 5 are the spectra for three different distances and the corresponding attenuation curve fit. Fibers are glued to the scintillator strip with Epotek which has a refractive index close to the scintillator's one. In Table 1 are the values of λ_1 and λ_2 for Bicron (B) and Kuraray (K) fibers. It can be seen that, besides fiber type, the gluing to the groove is an important factor.

Fiber Type	λ_1 m	λ_2 m
B (with epotek)	0.44	8.57
K (without epotek)	0.98	5.76

Table 1: Short and long components of attenuation length with Bicron and Kuraray fibers.

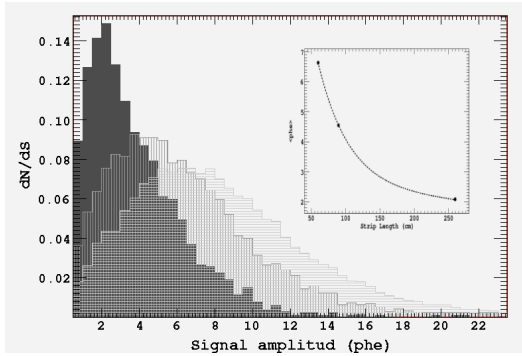


Figure 5: Measured charge spectra (in photoelectrons units) for a Bicron fiber at 60 cm, 90 cm and 260 cm.

Simulations

As mentioned in Section 2, full Monte Carlo simulations are needed to select the depth of each detector plane in order to optimize the discrimination potential between tracks belonging to electromagnetic particles and muons. This requires the simulation of the propagation of shower particles through the atmosphere and underground up to the planes, as well as the response of the scintillator strips to the passage of charged particles. Complete details of the end-to-end simulations can be found in [2]. We show here some result of the Geant4 [3] code implemented to simulate our detector. Figure 6 is a simplified visualization of a simulated muon crossing one detector strip. As can be noted, when a charged particle enters the scintillator many photons are produced. After a few reflections off the TiO_2 cover, some of them are absorbed and re-emitted by the wavelength shifter fiber and a small fraction arrives to the PMT. The

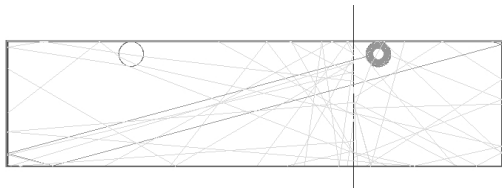


Figure 6: Simplified visualization of a simulated muon crossing a scintillator strip.

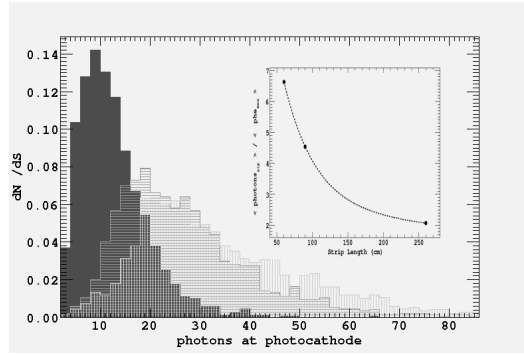


Figure 7: Simulated charge (in photons that hit the PMT cathode units) spectra for Bicron fiber at 60 cm, 90 cm and 260 cm.

various parameters characterizing the simulations are tuned to reproduce the features we measured in the laboratory. In particular, Figure 7 shows the longitudinal response of a Bicron-like simulated strip. As can be noted, the agreement with the corresponding real case, shown in Figure 5, is good.

Conclusions

We presented a muon telescope that is being built at present at ICN-UNAM, and that will be used to independently characterize the muon and electromagnetic components at ground level and to assess the magnitude of the tails of the electromagnetic distribution functions in extensive air shower. An additional goal is to measure the muonic to electromagnetic shower component ratio as a function of the depth underground. It is planned to operate for primary cosmic rays of energy above 6 PeV.

References

- [1] T. M. Collaboration, MINOS Technical Design Report, FNAL internal document NuMI-L-337, 1998.
- [2] F. Sanchez et al., , in: 30th ICRC, Merida, Mexico, 2007, 2007.
- [3] S. Agostinelli et al., , NIM (Phys. Res. Section 506 (2003) 250.